

# Modeling, Simulation, and Analysis of Permanent-Magnet Motor Drives, Part II: The Brushless DC Motor Drive

PRAGASEN PILLAY, MEMBER, IEEE, AND RAMU KRISHNAN, MEMBER, IEEE

**Abstract**—The brushless dc motor has a permanent-magnet rotor, and the stator windings are wound such that the back electromotive force (EMF) is trapezoidal. It therefore requires rectangular-shaped stator phase currents to produce constant torque. The trapezoidal back EMF implies that the mutual inductance between the stator and rotor is nonsinusoidal. Therefore, no particular advantage exists in transforming the machine equations into the well-known two-axis equations, which is done in the case of machines with sinusoidal back EMF's. This second part of the two-part paper develops a phase variable model of the BDCM and uses it to examine the performance of a BDCM speed servo drive system when fed by hysteresis and pulsewidth-modulated (PWM) current controllers. Transients similar to those applied to the permanent-magnet synchronous motor system of Part I are applied to this drive system to allow a comparative evaluation. Particular attention is paid to the motor torque pulsations. Some experimental verification is given.

## I. INTRODUCTION

THE ac servo has established itself as a serious competitor to the brush-type dc servo for industrial applications. In the fractional-to-30-hp range, the available ac servos include the induction, permanent-magnet synchronous, and brushless dc motors (BDCM) [1]. The BDCM has a trapezoidal back EMF, and rectangular stator currents are needed to produce a constant electric torque, as shown in Fig. 1. Typically, hysteresis or pulsewidth-modulated (PWM) current controllers are used to maintain the actual currents flowing into the motor as close as possible to the rectangular reference values. Although some steady-state analysis has been done [2], [3], the modeling, detailed simulation, and experimental verification of this servo drive has been neglected in the literature. The purpose of this paper is to fill this void.

It is shown that, because of the trapezoidal back EMF and the consequent nonsinusoidal variation of the motor inductances with rotor angle, a transformation of the machine equations to the well-known  $d, q$  model is not necessarily the best approach for modeling and simulation. Instead, the natural or phase variable approach offers many advantages.

Paper IPCSD 88-23, approved by the Industrial Drives Committee of the IEEE Industry Applications Society for presentation at the 1987 Industry Applications Society Annual Meeting, Atlanta, GA, October 19-23. Manuscript released for publication July 12, 1988.

P. Pillay was with the Electrical Engineering Department, Virginia Polytechnic Institute and State University, Blacksburg, VA. He is now with the Department of Electrical and Electronic Engineering, The University of Newcastle-upon-Tyne, Merz Court, Newcastle-upon-Tyne, England NE1 7RU.

R. Krishnan is with the Electrical Engineering Department, Virginia Polytechnic Institute and State University, Blacksburg, VA 24061.

IEEE Log Number 8825303.

While this approach has already been proposed, the back EMF is not represented as a Fourier series as is done in [4]. Instead, the back EMF is generated according to the position of the rotor using piecewise linear curves. This technique avoids the so-called Gibbs phenomenon that occurs due to the truncation of the higher order harmonics necessary when using the Fourier series approach.

Using this model of the BDCM, a detailed simulation and analysis of a BDCM speed servo drive is given. The simulation includes the state variable model of the motor and speed controller and a real-time model of the inverter switches. Although the switches are assumed to be ideal devices, the software developed is flexible enough to incorporate their turn-on and turn-off times. Every instance of a power switch opening or closing is simulated to determine the current oscillations and consequent torque pulsations. The effects of the hysteresis window size on the motor torque pulsations is investigated, and the effects of hysteresis and PWM current controllers on the drive system performance are also examined. Similar transients that were applied to the permanent-magnet synchronous motor (PMSM) drive in Part I [7] are applied here for comparative evaluation. In addition, both the small and large signal performances are investigated. Experimental verification is provided.

The paper is organized as follows. The mathematical model of the BDCM is developed in Section II. The operation of the hysteresis and PWM current controllers and the structure of the drive system are presented in Section III. The results and conclusions are in Sections IV and V, respectively.

## II. MATHEMATICAL MODEL OF THE BRUSHLESS DC MOTOR

The BDCM has three stator windings and permanent magnets on the rotor. Since both the magnet and the stainless-steel retaining sleeves have high resistivity, rotor-induced currents can be neglected and no damper windings are modeled. Hence the circuit equations of the three windings in phase variables are

$$\begin{bmatrix} v_a \\ v_b \\ v_c \end{bmatrix} = \begin{bmatrix} R & 0 & 0 \\ 0 & R & 0 \\ 0 & 0 & R \end{bmatrix} \begin{bmatrix} i_a \\ i_b \\ i_c \end{bmatrix} + p \begin{bmatrix} L_a & L_{ba} & L_{ca} \\ L_{ba} & L_b & L_{cb} \\ L_{ca} & L_{cb} & L_c \end{bmatrix} \begin{bmatrix} i_a \\ i_b \\ i_c \end{bmatrix} + \begin{bmatrix} e_a \\ e_b \\ e_c \end{bmatrix} \quad (1)$$

where it has been assumed that the stator resistances of all the windings are equal. (Symbols are defined in the Nomenclature at the end of the paper.) The back EMF's  $e_a$ ,  $e_b$ , and  $e_c$  have trapezoidal shapes as shown in Fig. 1. Assuming further that there is no change in the rotor reluctances with angle, then

$$L_a = L_b = L_c = L$$

$$L_{ab} = L_{ca} = L_{cb} = M.$$

Hence

$$\begin{bmatrix} v_a \\ v_b \\ v_c \end{bmatrix} = \begin{bmatrix} R & 0 & 0 \\ 0 & R & 0 \\ 0 & 0 & R \end{bmatrix} \begin{bmatrix} i_a \\ i_b \\ i_c \end{bmatrix} + \begin{bmatrix} L & M & M \\ M & L & M \\ M & M & L \end{bmatrix} p \begin{bmatrix} i_a \\ i_b \\ i_c \end{bmatrix} + \begin{bmatrix} e_a \\ e_b \\ e_c \end{bmatrix}, \quad (2)$$

but

$$i_a + i_b + i_c = 0. \quad (3)$$

Therefore,

$$Mi_b + Mi_c = -Mi_a. \quad (4)$$

Hence

$$\begin{bmatrix} v_a \\ v_b \\ v_c \end{bmatrix} = \begin{bmatrix} R & 0 & 0 \\ 0 & R & 0 \\ 0 & 0 & R \end{bmatrix} \begin{bmatrix} i_a \\ i_b \\ i_c \end{bmatrix} + \begin{bmatrix} L-M & 0 & 0 \\ 0 & L-M & 0 \\ 0 & 0 & L-M \end{bmatrix} p \begin{bmatrix} i_a \\ i_b \\ i_c \end{bmatrix} + \begin{bmatrix} e_a \\ e_b \\ e_c \end{bmatrix}. \quad (5)$$

In state-space form the equations are arranged as follows:

$$p \begin{bmatrix} i_a \\ i_b \\ i_c \end{bmatrix} = \begin{bmatrix} 1/(L-M) & 0 & 0 \\ 0 & 1/(L-M) & 0 \\ 0 & 0 & 1/(L-M) \end{bmatrix} \begin{bmatrix} i_a \\ i_b \\ i_c \end{bmatrix} + \begin{bmatrix} v_a \\ v_b \\ v_c \end{bmatrix} - \begin{bmatrix} R & 0 & 0 \\ 0 & R & 0 \\ 0 & 0 & R \end{bmatrix} \begin{bmatrix} i_a \\ i_b \\ i_c \end{bmatrix} - \begin{bmatrix} e_a \\ e_b \\ e_c \end{bmatrix} \quad (6)$$

and the electromagnetic torque is

$$T_e = (e_a i_a + e_b i_b + e_c i_c) / \omega_r. \quad (7)$$

The equation of motion is

$$p\omega_r = (T_e - T_L - B\omega_r) / J. \quad (8)$$

The currents  $i_a$ ,  $i_b$ , and  $i_c$  needed to produce a steady torque without torque pulsations are shown in Fig. 1. With ac machines that have sinusoidal back EMF's, a transformation can be made from the phase variables to  $d$ ,  $q$  coordinates either in the stationary, rotor, or synchronously rotating reference frames. Inductances that vary sinusoidally in the  $a$ ,  $b$ ,  $c$  frame become constants in the  $d$ ,  $q$  reference frame. The back EMF being nonsinusoidal in the BDCM means that the mutual inductance between the stator and rotor is nonsinu-

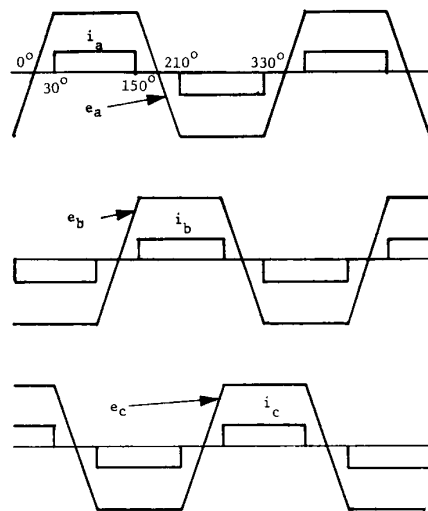


Fig. 1. Back EMF and current waveforms of brushless dc motor.

soidal, hence transformation to a  $d$ ,  $q$  reference frame cannot be easily accomplished. A possibility is to find a Fourier series of the back EMF, in which case the back EMF in the  $d$ ,  $q$  reference frame would also consist of many terms. This is considered too cumbersome, hence the  $a$ ,  $b$ ,  $c$  phase variable model already developed will be used without further transformation.

### III. CURRENT CONTROLLERS AND DRIVE SYSTEM

The power circuit and switching logic of the hysteresis current controller that drives the BDCM is exactly the same as that for the PMSM drive in Part I [7], and the reader is referred to [7, section IV] for the details. The only difference is in the shape of the reference current, which is sinusoidal for the PMSM but rectangular for the BDCM, as shown in Fig. 2.

Because of the nonzero inductance of the stator phase windings, the actual phase currents are unable to assume the desired rectangular form. Instead, the currents are trapezoidal due to the finite rise time. This has consequences on the torque production and the drive performance. This will be elaborated upon in Section IV.

A second method used to generate the required stator currents is to use a PWM current controller. The logic for this is exactly the same as that for the PMSM drive, and the reader is referred to [7, section V] for the relevant description.

The structure of the BDCM drive system is somewhat similar to that of the PMSM system in [7, fig. 5] with some differences that have been explained in [5]. The BDCM would probably not be used for extended speed operation because of its limited flux weakening capabilities, and hence the blocks associated with FW in [7, fig. 5] would not be necessary. In addition, since  $d$ ,  $q$  modeling is not used in the BDCM drive, the torque reference divided by the torque constant  $K_t$  would give a reference stator current  $i_s^*$  instead of the  $i_q^*$  shown in [7]. The rest of the drive system is essentially the same except that a resolver is not absolutely necessary for a BDCM speed servo. Hall-effect position sensors located every  $60^\circ$  (electrical) would suffice.

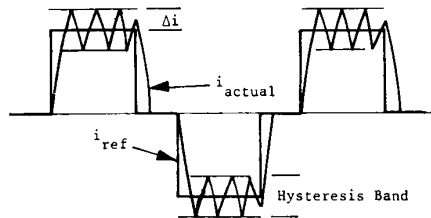


Fig. 2. Hysteresis current controller.

#### IV. RESULTS

Digital computer simulations of the entire BDCM drive system are presented in this section. The state space model of the BDCM and speed controller and switching logic of the current controllers are included in the simulation. Every instance of a power device switching on or off is modeled. Although the turn-on and turn-off times of the power devices are neglected, the simulation program developed is flexible enough to incorporate this. A proportional-integral (P-I) speed controller is used. Large and small signal transients are considered, and in addition, a comparison between the PWM and hysteresis current controllers on the drive performance is made. The BDCM drive is run through transients similar to those of the PWSM drive in Part I [7] so that a comparative evaluation can be made.

Fig. 3 shows key results when a BDCM (see Table I for the parameters) is started up from standstill to a speed of 1250 r/min using a PWM current controller. The speed is slightly underdamped in the design used here and increases in a linear manner during the initial startup period when the torque is constant and equal to the maximum capability of the motor. This ensures that the machine runs up in the shortest time possible. Every time the stator current is commutated from one phase to another, a torque pulsation is generated. This torque pulsation may be troublesome at low speeds as it can affect the accuracy and repeatability of position servo performance. The magnitude of the pulsation depends on the operating current level. At 2-pu current, the pulsation is about twice that at 1-pu current. When the operating current is zero, so is the commutation induced torque pulsation. In addition to these pulsations, high-frequency torque pulsations also occur due to the current oscillations produced by the PWM current controller. These are of sufficiently high frequency that they are effectively filtered out by the rotor inertia. These high-frequency pulsations depend only on the PWM switching frequency, unlike the commutation induced pulsations which depend on the operating speed. The higher the number of poles of the machine, the higher is the frequency of the commutation induced pulsations for a given operating speed. This is an advantage for speed servo performance since the higher the frequency of the pulsation, the lower is the effect on the speed because of the low-pass filtering effect of the rotor. However, the number of pulsations increases with the number of poles, and it is this factor that can be critical for position servo performance. Care should therefore be taken in using this machine for position servos [6].

The phase voltage switches continuously in an effort to force the actual current to equal the commanded value. The

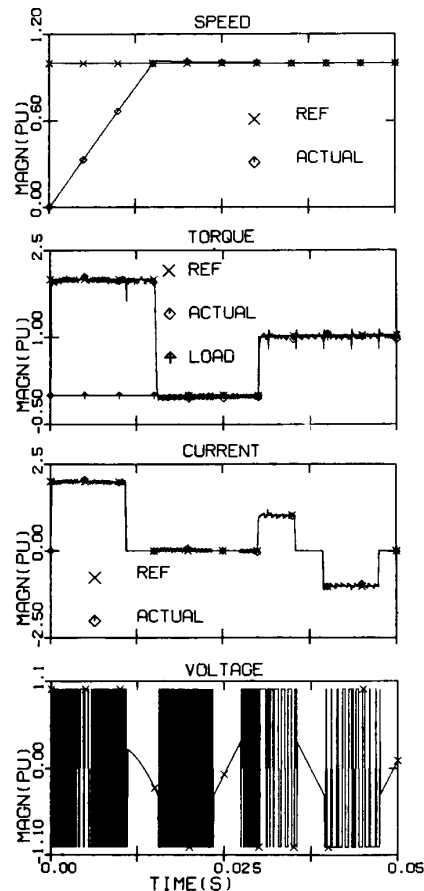


Fig. 3. Transients when fed from PWM current-source inverter (CSI).

TABLE I  
MOTOR PARAMETERS

$R$	0.29 $\Omega$
$L - M$	0.365 mH
$J$	0.0002265 $\text{kgm}^2$
$e_a/\omega_r$	0.185 V/rad/s

close tracking of the commanded current by the actual is evident except for the initial rise time due to the stator time constant. During the  $60^\circ$  period when the phase does not conduct current, no voltage is applied and the voltage visible across the motor terminals is the back EMF as shown in Fig. 3. This is unlike the PMSM drive results presented in Part I [7], where the voltage in any one phase is applied continuously to generate the sinusoidal currents needed for constant torque in that drive system.

At 0.03 s, a load of 1 pu is applied to the motor. This causes a small decrease in the speed as shown in Fig. 3. This decrease is barely perceptible and is less than the speed overshoot that occurred during the startup. The motor electric torque increases to 1 pu to satisfy the load torque requirements.

Fig. 4 shows the corresponding curves when a hysteresis instead of a PWM current controller is used. Clearly, the large signal speed transient is the same as when the PWM current controller is used. The voltage is used to force the currents to remain within the hysteresis bands. Although the oscillations

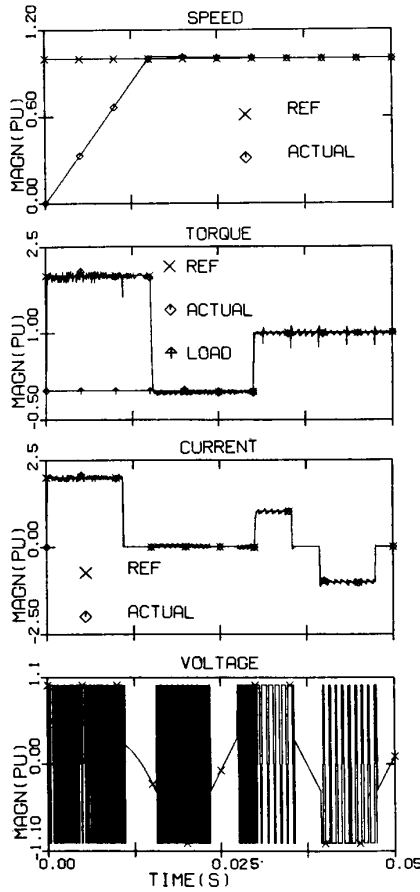


Fig. 4. Transients when fed from hysteresis CSI.

in the current, and consequently torque, are slightly larger with the hysteresis current controller, the average value of the torque is the same with both current controllers, thus producing the same large signal dynamics. By increasing the magnitude of the hysteresis bands, the resulting oscillations in current and subsequent torque pulsations are increased, as shown in Fig. 5. This also results in a reduction in the switching frequency of the inverter.

It is therefore clear that the speed transient is similar irrespective of whether a PWM or hysteresis current controller is used. However, if the hysteresis bands are so large as to produce large magnitude and low-frequency torque pulsations, then significant speed pulsations would occur.

The torque and current response, when a load torque of 0.1 pu is applied are shown in Fig. 6. These are scaled-down versions of the curves corresponding to the load torque of 1 pu. This indicates that, provided the phase current is input according to the timing strategy in Fig. 1, the transfer function between the electric torque and current is linear and the small and large signal responses are similar. If this timing is lost, then the transfer function becomes nonlinear and the above would no longer be true. In the case of the PMSM drive in Part I [7], this transfer function is linear only under vector control.

Fig. 7 shows the speed, torque, and current for a 0.1-pu increase in the speed of the machine after it has run up. When

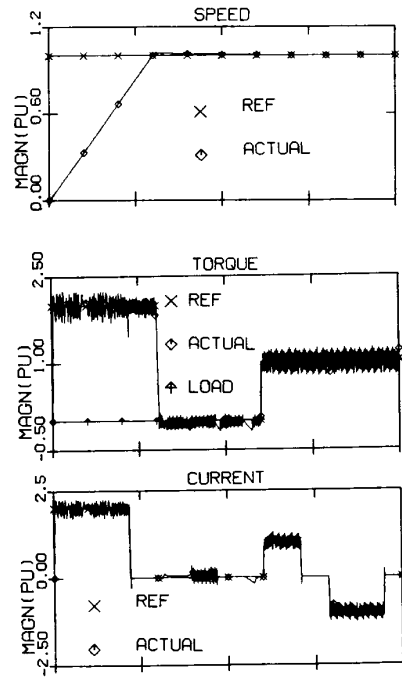


Fig. 5. Transients when fed from hysteresis CSI.

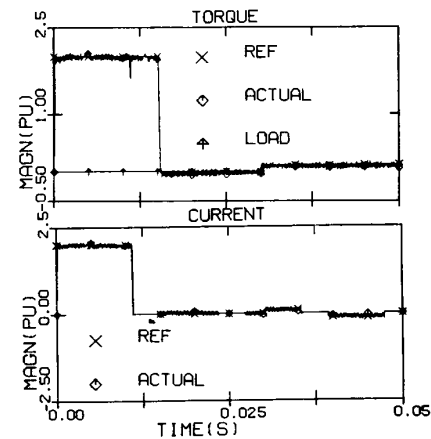


Fig. 6. Transients when fed from PWM CSI.

the speed command is input, a pulse of torque is demanded to increase the actual speed of the motor. This is provided by an increase in the rectangular current as shown in Fig. 7. In the PMSM drive, a pulse of sinusoidal current is demanded for the same purpose. Up to now transient results have been presented. Steady-state results are presented next.

From the results presented earlier, the motor torque pulsations clearly increase as a function of the hysteresis window size. This trend is plotted in Fig. 8 in pu. The relationship between the magnitude of the motor torque pulsations and the hysteresis window size is nonlinear, unlike the PMSM drive [7], where this relationship is linear. This result was obtained by varying the hysteresis window size and determining the corresponding torque pulsations.

From the previous results, it is also clear that the magnitude

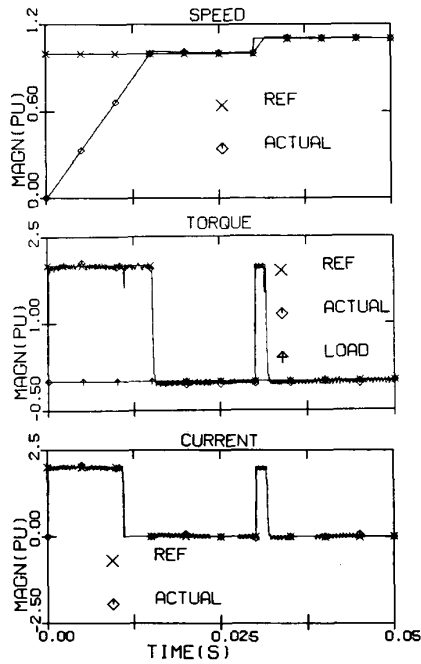


Fig. 7. Transients for 0.1 increase in speed.

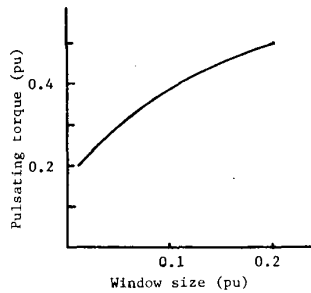


Fig. 8. Torque pulsations versus window size.

of the commutation-induced torque pulsation depends on the operating current level. In other words, the commutation-induced torque ripple depends on the current being commutated. This relationship is plotted in Fig. 9. The torque pulsation depends linearly on the current being commutated.

Decreasing the hysteresis window size increases the operating frequency of the inverter. This trend depends on the motor parameters and is somewhat similar to that presented in [7] and will therefore not be presented here.

From Fig. 3 it can be seen that the torque pulsations due to the current controller is extremely small, and its effect on the speed is not even noticeable. Just as in the PMSM drive in Part I, changing the PWM switching frequency does not affect the torque pulsations as much as varying the window size in the hysteresis current controller. Hence the PWM switching frequency should be chosen on the basis of the torque bandwidth and inverter switching capability rather than on the resulting torque pulsations, which is the same result as for the PMSM drive.

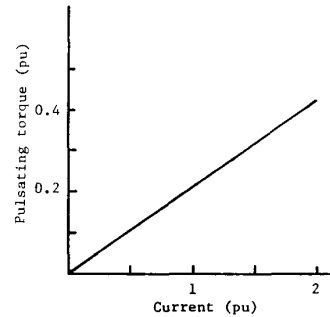


Fig. 9. Commutation torque pulsation versus current.

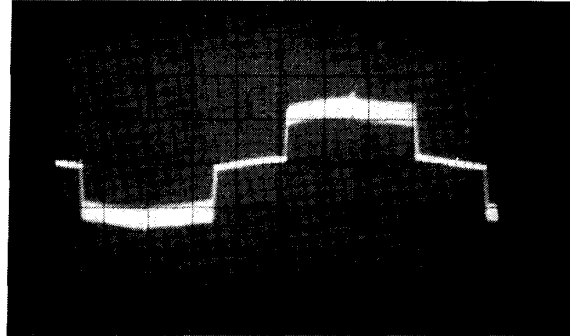


Fig. 10. Measured current of BDCM. X axis: 1 ms/div. Y axis: 2.5 A/div.

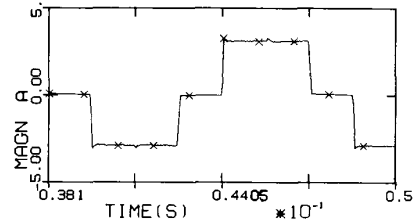


Fig. 11. Predicted current of BDCM.

### Experimental Verification

Fig. 10 shows the current waveform of the BDCM, thus verifying the rectangular shape. The prediction is in Fig. 11. The 120° conducting and 60° nonconducting periods can also be seen. To test the model developed, the machine was started up on an inertia load and its speed measured as shown in Fig. 12. The theoretical prediction of this speed is given in Fig. 13. The theoretical predictions and the practical measurements compare favorably, thus verifying that the model and computer simulation program used in this investigation is valid for the machine used.

### V. CONCLUSION

This part of the two-part paper has presented the modeling, simulation, and analysis of a BDCM drive. Particular attention was paid to the motor large- and small-signal dynamics and motor torque pulsations. The simulation included the state space model of the motor and speed controller and real-time model of the inverter switches. Every instance of a power

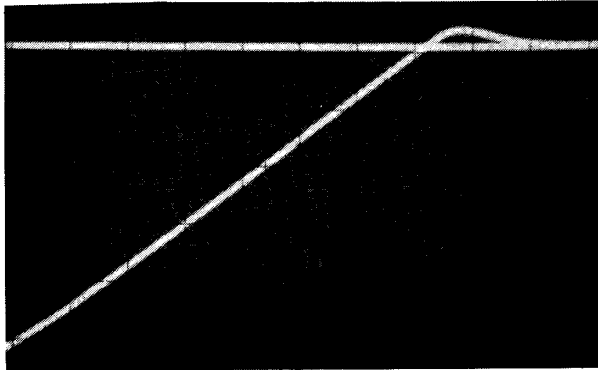


Fig. 12. Measured speed of BDCM. X axis: 10 ms/div. Y axis: 214 r/min/div.

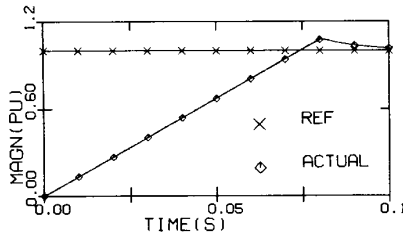


Fig. 13. Predicted speed of BDCM.

device turning on or off was simulated to calculate the current oscillations and resulting torque pulsations.

The results indicate that the small and large signal responses are very similar. This result is only true when the timing of the input phase currents with the back EMF is correct. In the case of the PMSM drive presented in Part I [7], this result is true under vector control. The large- and small-signal speed response is the same whether PWM or hysteresis current controllers are used. This is because, even though the torque pulsations may be different due to the use of different current controllers, the average value which determines the overall speed response is the same.

The relationship between the motor torque pulsations produced as a result of the hysteresis current controller and the window size is nonlinear, unlike the PMSM drive, where it is linear. The relationship between the commutation-induced torque pulsation and the current being commutated, however, is linear. This has implications in position applications. The accuracy and repeatability of position servo performance can be affected, particularly if high currents are commanded.

The frequency of the commutation-induced torque pulsations increase as the number of poles of the machine is increased, thus reducing their effects on the speed. A high pole number is therefore advantageous in a speed servo. However, since the number of pulsations increase with an increase in the number of poles for a given mechanical rotation, a very high pole number may be undesirable for position servo performance.

NOMENCLATURE

- $e_a, e_b, e_c$   $a, b,$  and  $c$  phase back-EMF's, V
- $E_p$  Peak value of back-EMF, V.
- $K_t$   $= 2e_a/\omega_r$ , torque constant.
- $L_a, L_b, L_c$  Self-inductance of  $a, b,$  and  $c$  phases, H.
- $L_{ab}$  Mutual inductance between phase  $a$  and  $b$ , H.
- $v_a, v_b, v_c$   $a, b,$  and  $c$  phase voltages, V.

Other symbols used are listed in [7].

ACKNOWLEDGMENT

The authors would like to thank Inland Motor, Specialty Products Division, Kollmorgen Corporation, of Radford Virginia for the loan of one of their BDCM drives.

REFERENCES

- [1] R. Krishnan, "Selection criteria for servo motor drives," in *Proc. IEEE IAS Annu. Meeting*, 1986, pp. 301-308.
- [2] T. M. Jahns, "Torque production in permanent-magnet synchronous motor drives with rectangular current excitation," *IEEE Trans. Ind. Appl.*, vol. IA-20, no. 4, pp. 803-813, July/Aug. 1984.
- [3] S. Funabiki and T. Himei, "Estimation of torque pulsation due to the behavior of a converter and an inverter in a brushless dc-drive system," *Proc. Inst. Elec. Eng.*, vol. 132, pt. B, no. 4, pp. 215-222, July 1985.
- [4] N. A. Demerdash and T. W. Nehl, "Dynamic modeling of brushless dc motors for aerospace actuation," *IEEE Trans. Aerosp. Electron. Syst.*, vol. AES-16, no. 6, pp. 811-821, Nov. 1980.
- [5] P. Pillay and R. Krishnan, "Application characteristics of permanent magnet synchronous and brushless dc motors for servo drives," in *Proc. 1987 IEEE IAS Annual Meeting*, Atlanta, GA, Oct. 19-23, pp. 380-390.
- [6] G. Pfaff, A. Weschta, and A. Wick, "Design and experimental results of a brushless ac servo-drive," in *Proc. IEEE IAS Annu. Meeting*, 1982, pp. 692-697.
- [7] P. Pillay and R. Krishnan, "Modeling, simulation and analysis of permanent magnet motor drives—Part I: The permanent magnet synchronous motor drive," this issue, pp. 265-273.

**Pragasen Pillay** (S'84-M'87), for a photograph and biography please see page 273 of this TRANSACTIONS.

**Ramu Krishnan** (S'81-M'82), for a photograph and biography please see page 273 of this TRANSACTIONS.